

We are IntechOpen, the world's leading publisher of Open Access books Built by scientists, for scientists

6,600

Open access books available

178,000

International authors and editors

195M

Downloads

Our authors are among the

154

Countries delivered to

TOP 1%

most cited scientists

12.2%

Contributors from top 500 universities



WEB OF SCIENCE™

Selection of our books indexed in the Book Citation Index
in Web of Science™ Core Collection (BKCI)

Interested in publishing with us?
Contact book.department@intechopen.com

Numbers displayed above are based on latest data collected.
For more information visit www.intechopen.com



Chapter

The Influence of Inclined Barriers on Airflow Over a High Speed Train under Crosswind Condition

Masoud Mohebbi, Yuan Ma and Rasul Mohebbi

Abstract

During the last decade the problem of crosswind has developed into an important subject amongst the topics in railway engineering. When high speed trains are exposed to extreme weather conditions such as intense lateral winds, storms and tornadoes, lateral loads acting on the train can cause overturning of the train. This present work analyzed the aerodynamic mechanism of a high-speed train with and without two inclined barriers. A three-dimensional numerical model of a train-barrier-crosswind system is adopted to investigate the effects of inclined angles of barriers on the flow patterns and the aerodynamic coefficients. This perusal surveys the design criteria indispensable for barriers that are installed alongside the tracks to protect the passing trains under strong side winds. By using a numerical code based on Lattice Boltzmann Method (LBM) it is attempted to initially investigate the behavior of airflow behind the barriers. Finally, it is found that the presence of the barriers has a great impact on decreasing the intensity of the air flow above the train. This study's findings could be utilized as a reference for practical usage of barriers in railway transportation.

Keywords: train aerodynamic, crosswind, high speed train, barrier, LBM

1. Introduction

The aerodynamic behaviour caused by the effect of crosswinds is one of the most serious challenges concerning the safety of high-speed trains [1–3]. The existence of crosswind would lead to the high-speed train being accompanied by a rather complicated flow field, that fluctuates both temporally and spatially. As a consequence, the train's aerodynamic properties are affected, and the running safety would be imperilled, especially when the train is through a bridge, the crosswinds become more complicated due to the bridge structure [4, 5]. Thus, the effects of crosswinds on aerodynamic behaviour are crucial.

With the fast growth of high-speed trains, the effect of crosswinds has become more and more prominent [6, 7]. To reduce the effects of crosswind, the typical windproof is widely used. It includes wind barriers and anti-wind open-cut tunnels. Wind barriers are simple and convenient devices, that are utilized in high-speed

tracks at strong crosswinds conditions. In recent years, many researchers have investigated the impact of wind barriers on the aerodynamic characteristics of a high-speed train. Deng et al. [8] numerically studied the windproof performance of wind barriers in the wind-vehicle-bridge system. They found that the wind barrier is exceedingly important and significantly affects the aerodynamic coefficient, flow structure, and traveling safety. Guo et al. [9] assessed the impact of wind barriers on the traveling safety of a high-speed train to crosswinds. They determined that the existence of the wind barriers causes negative effects on the bridge. Gu et al. [10] experimentally and numerically studied the aerodynamic characteristics of a train with various lengths of vertical wind barriers. They found that when the wind barrier length varies, the impact on the train's head is more obvious than on the tail.

Liu et al. [11] numerically studied the aerodynamic behaviour of a high-speed train running through a windbreak region while being buffeted by crosswinds. They found that when the train entered the region under the crosswind, the aerodynamic coefficients change suddenly. Zou et al. [12] performed a numerical simulation to evaluate the effect of wind barriers of a high-speed train on a bridge. In their work, two vertical wind barriers were placed on either sides of the railway. Xiang et al. [13] executed a wind tunnel testing to evaluate the aerodynamic load of a high-speed train. Their findings revealed that a wind barrier of a specific height increases lift. However, it is still indistinct how the inclined angle of the barriers affects the flow pattern around the train and barriers, which benefits the development of high-speed trains. Therefore, the present work seeks to explore the mechanisms of the impacts of barriers inclined angles on the high-speed train and explain the relationships between the barriers with different inclined angles and the train.

For investigating the effects of barriers on the train aerodynamic mechanism, there are four approaches, including analytical method, numerical simulation, field measurement, and wind tunnel test. In the work of Yang et al. [14], the Finite Volume Method (FVM) in ANSYS FLUENT software was used to solve the 3D unstable incompressible Navier-Stokes equations. Catanzaro et al. [15] compared the CFD results and wind-tunnel tests of a high-speed train in a crosswind. They found that the results of the stationary model become more different from the moving model and the environment has a major impact on the train's incoming flow. Wang et al. [16] conducted an experiment work to study the influences of crosswinds on the aerodynamic properties of a high-speed train.

As a recognized and powerful numerical method, the Lattice Boltzmann approach has been widely utilised to simulate fluid flow and heat transfer problems [17, 18]. The Lattice Boltzmann equation was created and developed as a computational alternative to the solving the Navier-Stokes equations of continuum fluid physics [19]. Due to the advantages of LBM, such as its ability to dealing with complicated boundaries, parallelize the algorithm, and incorporating microscopic interactions, it has also been used to model the aerodynamic behaviours of the high-speed train. Mohebbi and Rezvani [20] utilized LBM to investigate the consequences of windbreaks geometry on two-dimensional airflow past a high-speed train. They determined that the performance of windbreak is significantly dependent on its height and edge angle. The LBM was also used by Wang et al. [21] to predict the aerodynamic behaviour of a high-speed train. They concluded that LBM has many advantages compared with the traditional CFD method. In the previous work, the authors [22] assessed the impact of porous shelters alongside a high-speed track on the vehicle's aerodynamic behaviour and the modelling was conducted utilizing the lattice Boltzmann method. The authors

have proved that the LBM codes with smaller lattices can provide a reasonable accuracy result.

To the best of the authors' knowledge, the effects of two inclined barriers on the aerodynamic mechanism of a train have never been studied. In the present work, the German Intercity Express (ICE3) high-speed train was focused and a three-dimensional numerical model of the train-barrier-crosswind system is adopted to investigate the effect of two inclined barriers on the train's aerodynamic mechanism through the Lattice Boltzmann method. The effect of barrier inclined angle and direction on the velocity, pressure, turbulence intensity, streamlines, and aerodynamic coefficients are investigated.

2. The model description

Figure 1 shows the geometry under consideration in the present work. The height of the ICE3 high-speed train (H_{Train}) is 3.5 m. Two barriers are set on the right and left sides, respectively. The distance between the two barriers ($L_{Barrier\ Distance}$) is 14 m. The spacing between the barrier and the boundary of the calculation domain is $10H_{Train}$, which is the same as the height of the computational domain. The wind blows parallel to ground level from the right to the left, with a uniform velocity of 80 m/s. The height and width of the calculation domain are $10H_{Train}$ and $2H_{Train}$, respectively. Besides, the forces and momentums concerning the coordinate system's directions (x, y, z) are specified by the European Standard EN14067-6 (**Figure 1**).

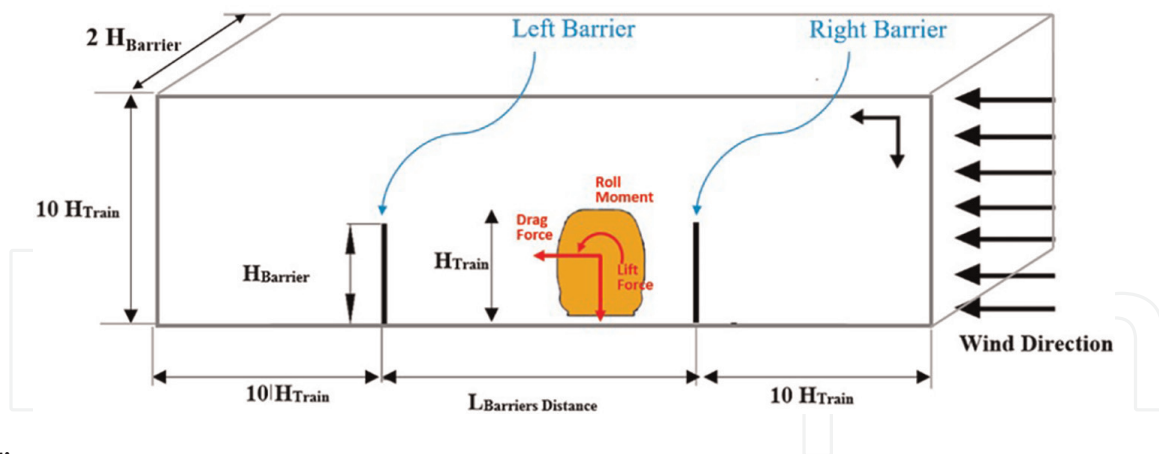


Figure 1.
 The computational domain and the aerodynamic coefficients definitions.



Figure 2.
 The model of considered geometry.

Type I: $\theta = 0^\circ$	Type II: $\theta = +2.5^\circ$	Type III: $\theta = +5.0^\circ$
Type IV: $\theta = +7.5^\circ$	Type V: $\theta = +10.0^\circ$	Type VI: $\theta = -2.5^\circ$
Type VII: $\theta = -5.00^\circ$	Type VIII: $\theta = -7.5^\circ$	Type IX: $\theta = -10.0^\circ$

Table 1.
The barrier types with different inclined angles.

In the present work, the effects of barriers are focused on. The heights of the two barriers ($H_{Barrier}$) are the same and $H_{Barrier} = 3.0$ m. As shown in **Figure 2**, the effect of barrier inclined angle (θ) is investigated in the present work. According to the different barrier inclined angles, nine types of cases are simulated (**Table 1**).

3. The numerical method

The Lattice Boltzmann Method is used in this paper to model fluid flow past a high-speed train with two barriers. The velocity of the two-dimensional nine-speed (D2Q9) model in multiple directions can be defined as [23]:

$$e_i = \begin{cases} (0, 0) & (i = 0) \\ \cos\left(\frac{i\pi}{2} - \frac{\pi}{2}\right), \sin\left(\frac{i\pi}{2} - \frac{\pi}{2}\right) \cdot c & (i = 1, \dots, 4) \\ \sqrt{2} \left(\cos\left(\frac{i\pi}{2} - \frac{9\pi}{4}\right), \sin\left(\frac{i\pi}{2} - \frac{9\pi}{4}\right) \right) \cdot c & (i = 5, \dots, 8) \end{cases} \quad (1)$$

where $c = \Delta x / \Delta t$ is the velocity of lattice, Δx is the lattice space, Δt is the time step and i is the different direction.

The governing equation in the lattice Boltzmann method is:

$$f_i(x + e_i \Delta t, t + \Delta t) = f_i(x, t) + \frac{\Delta t}{\tau_v} [f_i^{eq}(x, t) - f_i(x, t)] \quad (2)$$

where f_i is the distribution function and f_i^{eq} is the equilibrium distribution function, which can be calculated according to:

$$f_i^{eq} = w_i \rho \left[1 + \frac{e_i u}{c_s^2} + \frac{1}{2} \frac{(e_i u)^2}{c_s^4} - \frac{1}{2} \frac{u^2}{c_s^2} \right] \quad (3)$$

where w_i are the weights, $w_0 = 4/9$, $w_{1-4} = 1/9$, $w_{5-8} = 1/36$.

The distribution functions can be used to obtain the macroscopic variables,

$$\rho = \sum_i f_i \quad (4)$$

$$\rho u = \sum_i e_i f_i \quad (5)$$

With the multi-scaling expansion, the mass and the moment equations can be obtained:

$$\frac{\partial \rho}{\partial t} + \nabla \cdot (\rho u) = 0 \quad (6)$$

$$\frac{\partial \rho}{\partial t} + \nabla \cdot (\rho u u) = -\nabla P + \vartheta [\nabla^2 (\rho u) + \nabla (\nabla \cdot (\rho u))] \quad (7)$$

More information on the present numerical method can be found in the authors' previous paper [19].

In this study, Wall Modelled Large Eddy Simulation (WMLES) [24] approach was used to consider the turbulence. LES has been proved as a compliant numerical approach in computing and simulating unsteady turbulent flows. WMLES takes the wall models into account and its primary idea is that the near-wall turbulence length scales grow linearly with the wall distance, leading to the smaller and smaller eddies as the wall is approached.

The aerodynamic coefficients in terms of non-dimensional characteristics are described by EN 14067-1 as follows:

$$\text{Forces : } F = \frac{\rho U_{\infty}^2}{2} \cdot A \cdot C \quad (8)$$

$$\text{Momentums : } M = \frac{\rho U_{\infty}^2}{2} \cdot A \cdot l \cdot C \quad (9)$$

$$\text{Pressure : } P - P_{\infty} = \frac{\rho U_{\infty}^2}{2} \cdot C_p \quad (10)$$

U_{∞} is the free stream velocity, P is the local static pressure, and P_{∞} is the free-stream static pressure.

4. The grid independence and validation

For the validation of the current CFD code based on LBM, the aerodynamic force and moment coefficients are calculated to compare with the experimental wind tunnel works from EN 14067-6:2010, which is performed by Schober et al. [25]. **Table 2** shows the comparison of the aerodynamic coefficient by present code and the standard data. The high-speed train model with no barrier is tested and the drag, lift, and rolling moment coefficients have been calculated for comparison. It is clear to see that the disparity is acceptable, which validated the present code and results.

Mode	No-barrier		
	CFD	Standard	Error percentage CFD relative to standard (%)
Drag coefficient	0.33	0.38	-14
Lift coefficient	-4.86	-5.49	-11
Rolling moment coefficient	3.00	3.35	-11

Table 2.
 Verification with the standard EN 14067-6: 2010.

5. The results and discussion

In the present section, the effects of barriers with the inclined angle (nine types) on the flow field and aerodynamic forces and moments are discussed in form of velocity contours, velocity vectors, total pressure contours, turbulence intensity contours, and aerodynamic force.

Figure 3 shows the effects of barriers with the inclined angle on the velocity contours around the train. When there is no barrier, the high flow velocity can be found at the upper windward of the train as the flow approaches the train. A large low-velocity zone occurs on the leeward side, which is the left side due to the inflow direction. Meanwhile, the high-velocity gradient is generated on the top of the train. It is obvious that the flow velocity around the train is rather uneven, leading to a considerable negative influence on the stability of the train. As the barriers are introduced, the flow velocity around the train becomes more even, and the flow pattern changes substantially. When $\theta = 0^\circ$, the right barrier takes the place of the train to withstand the crosswind. As a result, the line of a large velocity gradient is formed

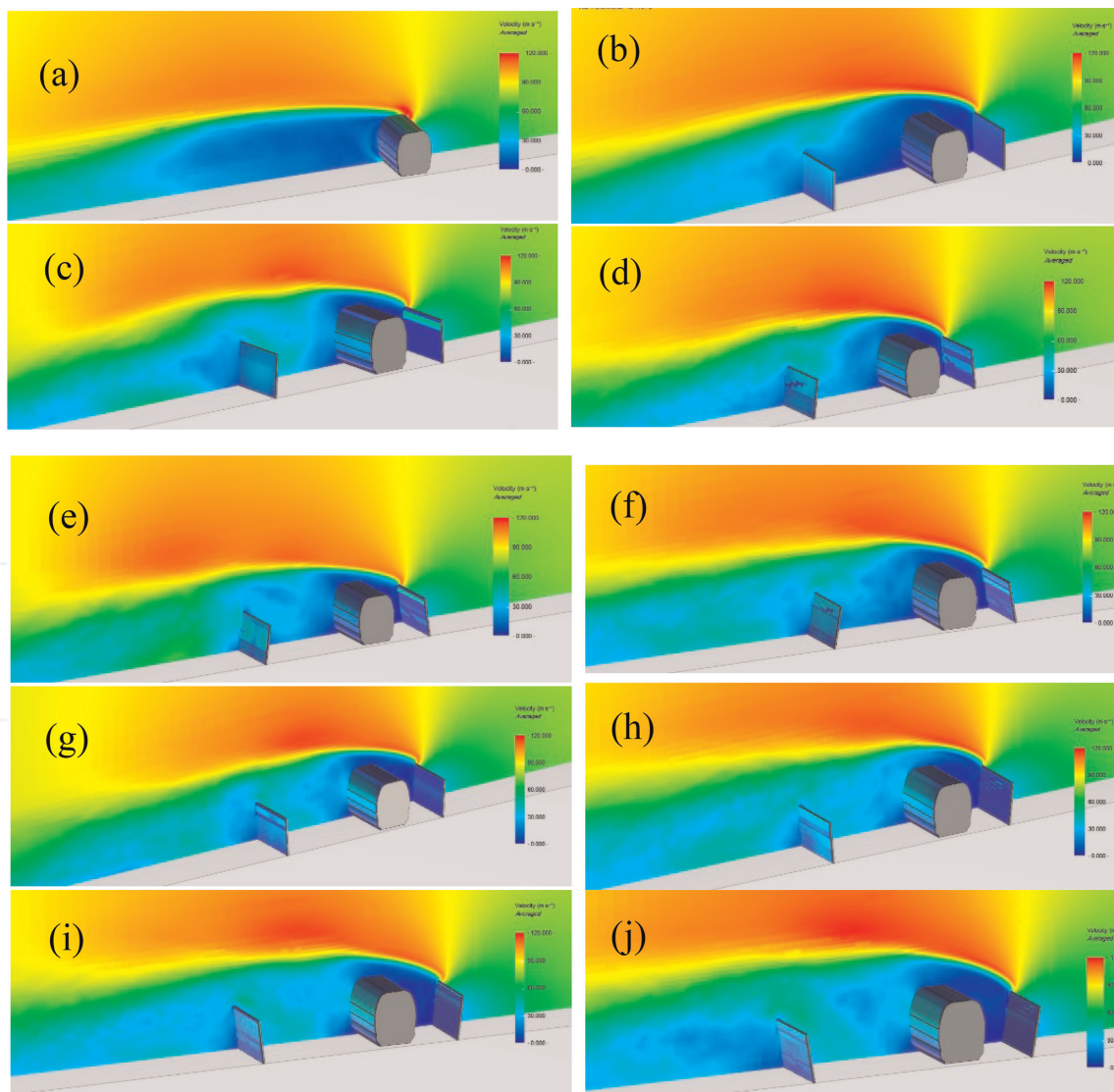


Figure 3. The velocity contours (a) without barriers, (b) $\theta = 0^\circ$, (c) $\theta = +2.5^\circ$, (d) $\theta = +5.0^\circ$, (e) $\theta = +7.5^\circ$, (f) $\theta = +10.0^\circ$, (g) $\theta = -2.5^\circ$, (h) $\theta = -5.0^\circ$, (i) $\theta = -7.5^\circ$, and (j) $\theta = -10.0^\circ$.

from the top side of the barrier. And the train is surrounded by the low-velocity air caused by the right barrier and the flow velocity around the train is almost even. However, when the angle changes to $\theta = +2.5^\circ$, $+5.0^\circ$, $+7.5^\circ$, and $+10.0^\circ$, the function of the right barrier mentioned above weakens. The area of the low-velocity region caused by the right barrier is reduced and the distribution of flow velocity on the left of the train becomes unequal correspondingly. As shown in **Figure 3g-j**, when the angle becomes a negative value, the flow velocity on the left side of the train increases and becomes larger than that without a barrier. As a result, the velocity unevenness of the flow field around the train is significantly increasing.

Figure 4 shows the velocity vectors around the train and barriers. Without the barriers, the flow separations happen from the train's leeward side and then leave the surface and are involved in the leeward vortex. When the barriers are induced, the flow separations begin from the barrier, and the train is surrounded by vortices. As a result, the difference in velocity between the left and right sides of the train decreases, and the velocity on the windward of the train is lower than that on the leeward. However, when the inclined angle changes from positive to negative, the velocity on the leeward of the train increases significantly.

To investigate the effect of barriers and inclined angles on the pressure of the train, **Figure 5** depicts the total pressure contours. Without the barrier, the pressure on the right side of the train is apparently higher than on the left side because of the

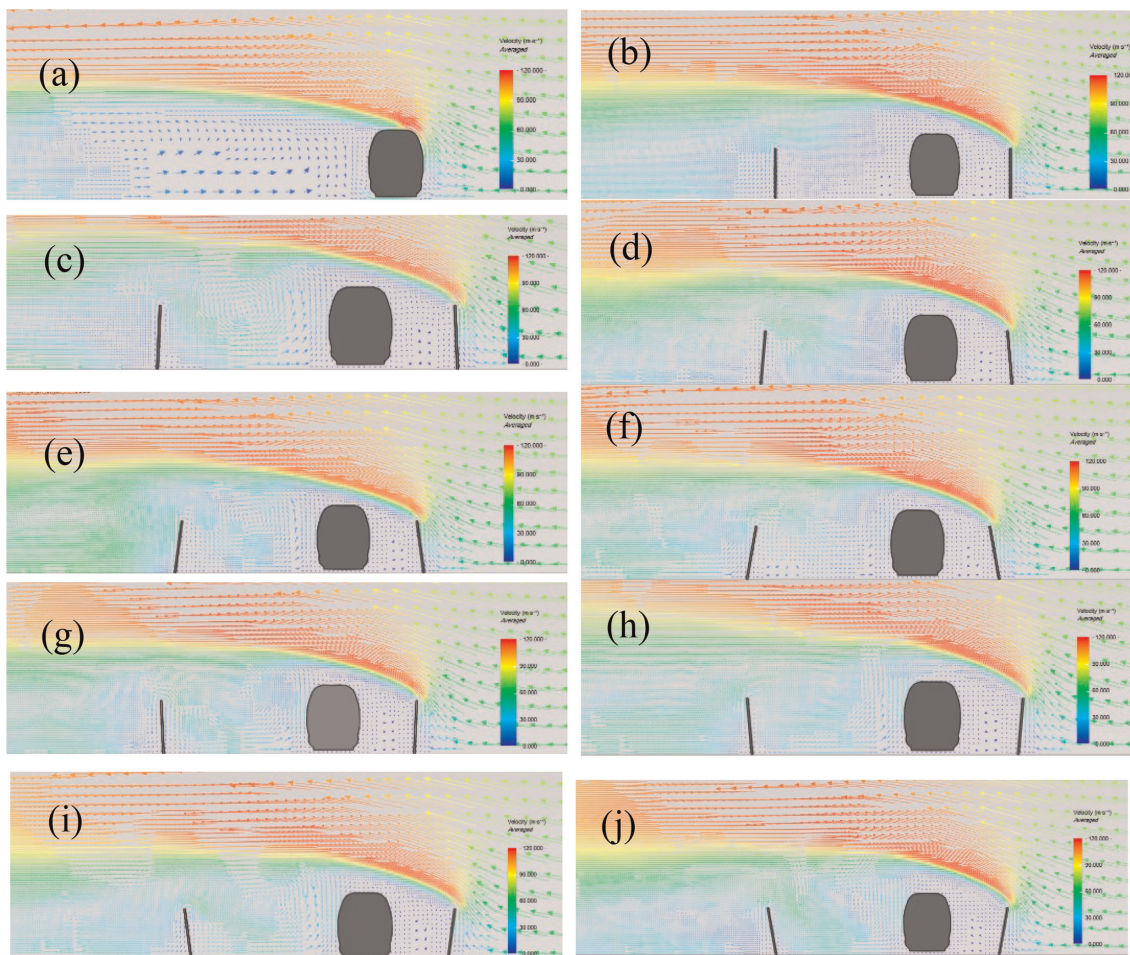


Figure 4. The velocity vectors (a) without barriers, (b) $\theta = 0^\circ$, (c) $\theta = +2.5^\circ$, (d) $\theta = +5.0^\circ$, (e) $\theta = +7.5^\circ$, (f) $\theta = +10.0^\circ$, (g) $\theta = -2.5^\circ$, (h) $\theta = -5.0^\circ$, (i) $\theta = -7.5^\circ$, and (j) $\theta = -10.0^\circ$.

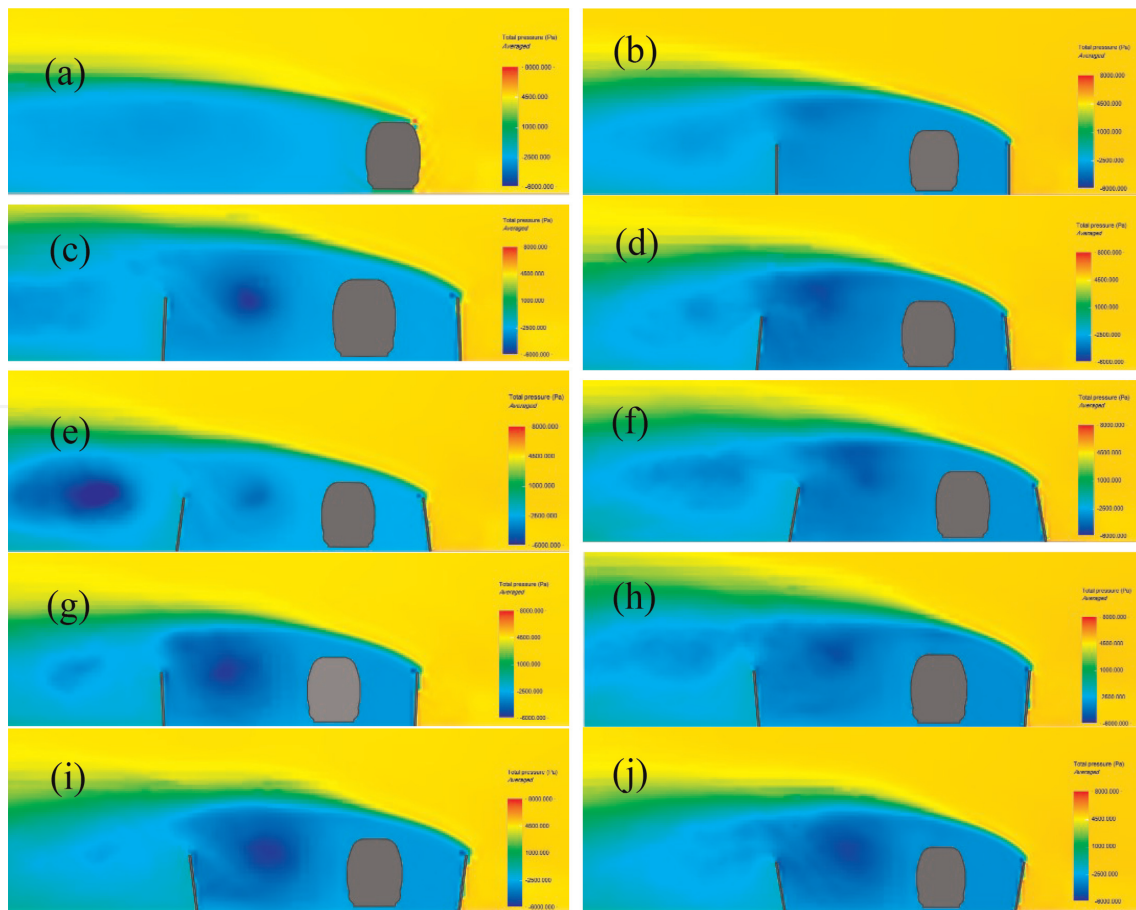


Figure 5. The total pressure contours (a) without barriers, (b) $\theta = 0^\circ$, (c) $\theta = +2.5^\circ$, (d) $\theta = +5.0^\circ$, (e) $\theta = +7.5^\circ$, (f) $\theta = +10.0^\circ$, (g) $\theta = -2.5^\circ$, (h) $\theta = -5.0^\circ$, (i) $\theta = -7.5^\circ$, and (j) $\theta = -10.0^\circ$.

crosswind. It should be stated that the pressure on the left side of the train is approximately identical. When two barriers with $\theta = 0^\circ$ are placed, a low-pressure zone is formed between two barriers. The pressure gradient in this low-pressure zone is small and the relatively low pressure occurs around the top of the left barrier. When the angle increases to $+2.5^\circ$, the pressure on the right side of the train increases slightly. However, there is one noticeable lower pressure region between the left barrier and the train, which also leads to the pressure gradient. When the inclined angles are negative value, as seen in **Figure 5g–f**, the area of the lower pressure region increase and occupies almost the whole zone between the left barrier and the train. Moreover, when the inclined angle of barriers varies, the pressure gradient between the train and the right barrier is always small.

To analyse the flow pattern characteristics, the turbulence intensity is calculated to show the turbulence level, which is presented in **Figure 6**. Firstly, the existence of the barriers and the inclined angle affect the flow pattern characteristics. Without the barriers, the high turbulence intensity occurs on the train's leeward side, and the turbulence intensity on the windward side is almost equal to 0. However, when two barriers with $\theta = 0^\circ$ are placed on both sides of the train, the turbulence intensity around the train is affected significantly. Both the windward and leeward sides experience a rise in turbulence intensity. The windward side, which is between the train and the right barrier, has larger turbulence intensity than the leeward side. Besides,

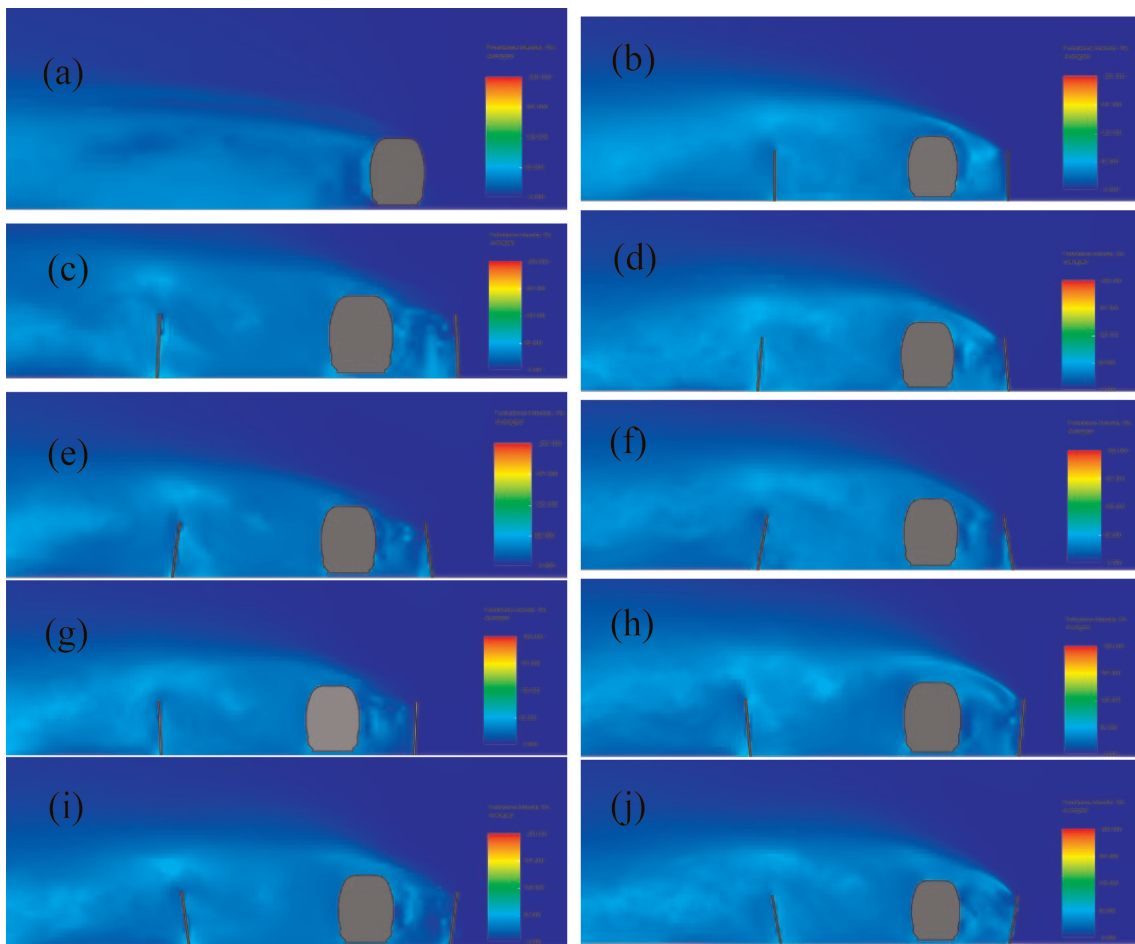


Figure 6. The turbulence intensity contours (a) without barriers, (b) $\theta = 0^\circ$, (c) $\theta = +2.5^\circ$, (d) $\theta = +5.0^\circ$, (e) $\theta = +7.5^\circ$, (f) $\theta = +10.0^\circ$, (g) $\theta = -2.5^\circ$, (h) $\theta = -5.0^\circ$, (i) $\theta = -7.5^\circ$, and (j) $\theta = -10.0^\circ$.

the turbulence intensity on the right side of the right barrier is adjacent to 0. As the barrier inclined angle increases to $+2.5^\circ$, the turbulence intensity decreases and the diminishment is more significant between the left barrier and the train, which shows the effect of barriers on the turbulence intensity difference on both sides. However, when the inclined angle increases to $+5.0^\circ$ and $+7.5^\circ$, the turbulence intensity difference between both sides decreases. That's to say, the difference between the leeward and windward sides of the train becomes small. When the inclined angle increases from $+7.5^\circ$ to $+10.0^\circ$, the difference increases and the turbulence intensity on the leeward of the train is slightly larger than on the windward. When the inclined angle becomes minus, the turbulence intensity changes slightly.

Figure 7 shows the effect of barrier inclined angle on the drag force coefficient, lift force coefficient, rolling moment coefficient, and lee-rail rolling moment coefficient. Firstly, it can be found that using the barriers with a positive inclined angle cannot decrease the drag coefficient. The barriers with zero or negative angles can decrease the drag coefficient. The barriers with a positive inclined angle cause a positive drag coefficient of the train, and the barriers with a negative angle lead to a negative value. Besides, the absolute value of the drag coefficient of positive angles is larger than those of negative ones. This can be analysed by comparing two types of barriers. The positive angles of barriers lead to the narrower space around the train. It should be

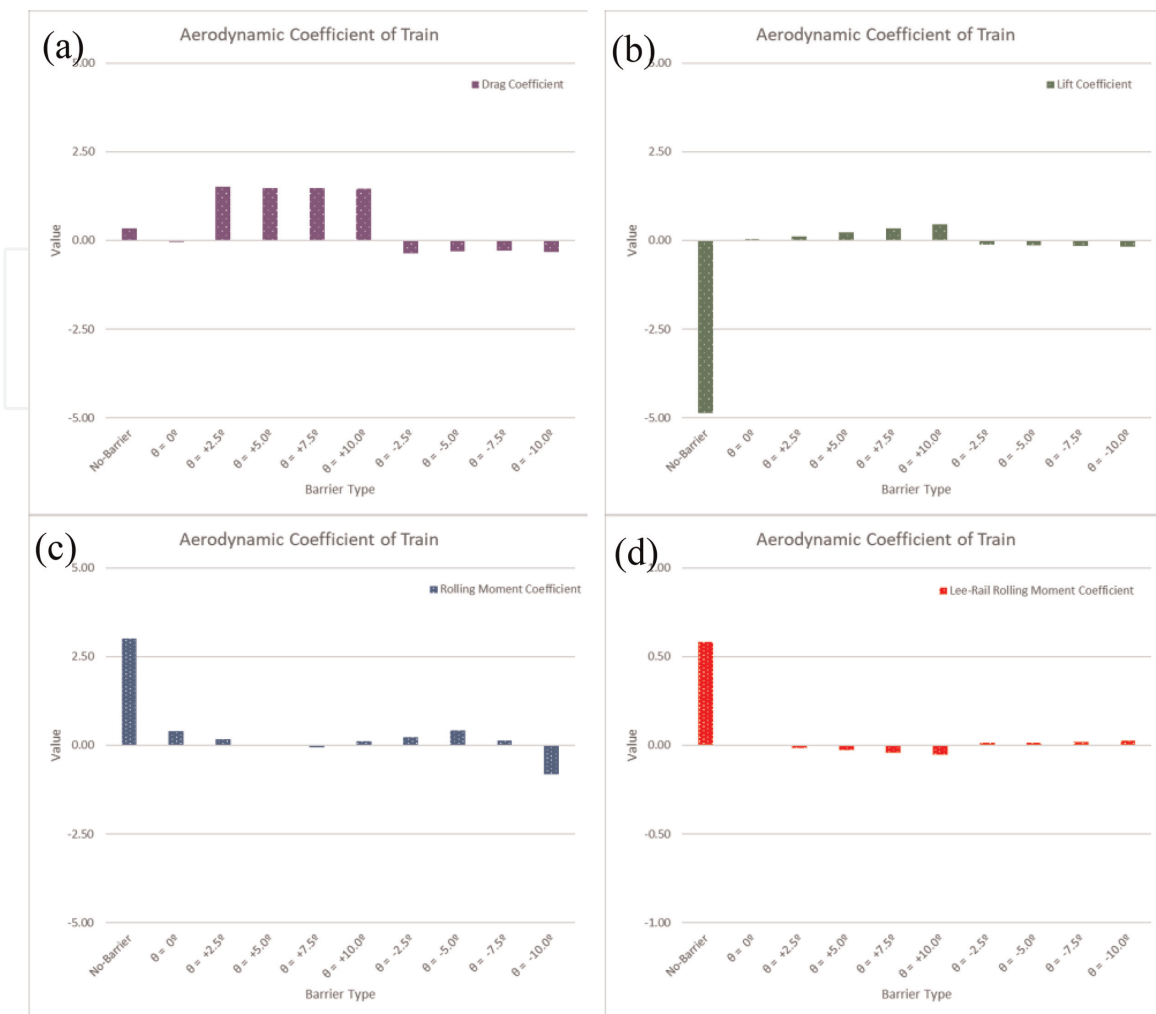


Figure 7. The aerodynamic coefficients: (a) drag force coefficient, (b) lift force coefficient, (c) rolling moment coefficient, and (d) lee-rail rolling moment coefficient.

stated that the barriers with zero inclined angle have the smallest value of drag coefficient. As for the lift coefficient, the existence of barriers is beneficial to the diminution of the lift coefficient regardless of the inclined angle. The zero inclined angles can cause the smallest lift coefficient. The barriers with positive angles lead to the positive value of the lift coefficient and the negative angles cause the negative value, which is similar to the effect on the drag coefficient. Concerning the rolling moment and the lee-rail rolling moment coefficients, the presence of barriers can decrease them. These parameters are important for the train, which is because they are answerable for the loading and unloading of wheelsets. It is obvious that the existence of barriers with any inclined angles, including zero, can decrease the rolling and lee-rail rolling moment coefficients. As the inclined angle of the barrier become $\theta = +5.0^\circ$, the value of the rolling moment coefficient become the minimum. And then when the angle increases, the value also increases. The effect of inclined angle on the lee-rail rolling moment coefficient is more distinct. The positive inclined angle leads to the negative lee-rail rolling moment coefficient and the negative angle cause the positive coefficient.

To demonstrate the impact of various types of barriers (with barriers or not, barriers inclined angle), the effects of barrier type on aerodynamic coefficients are

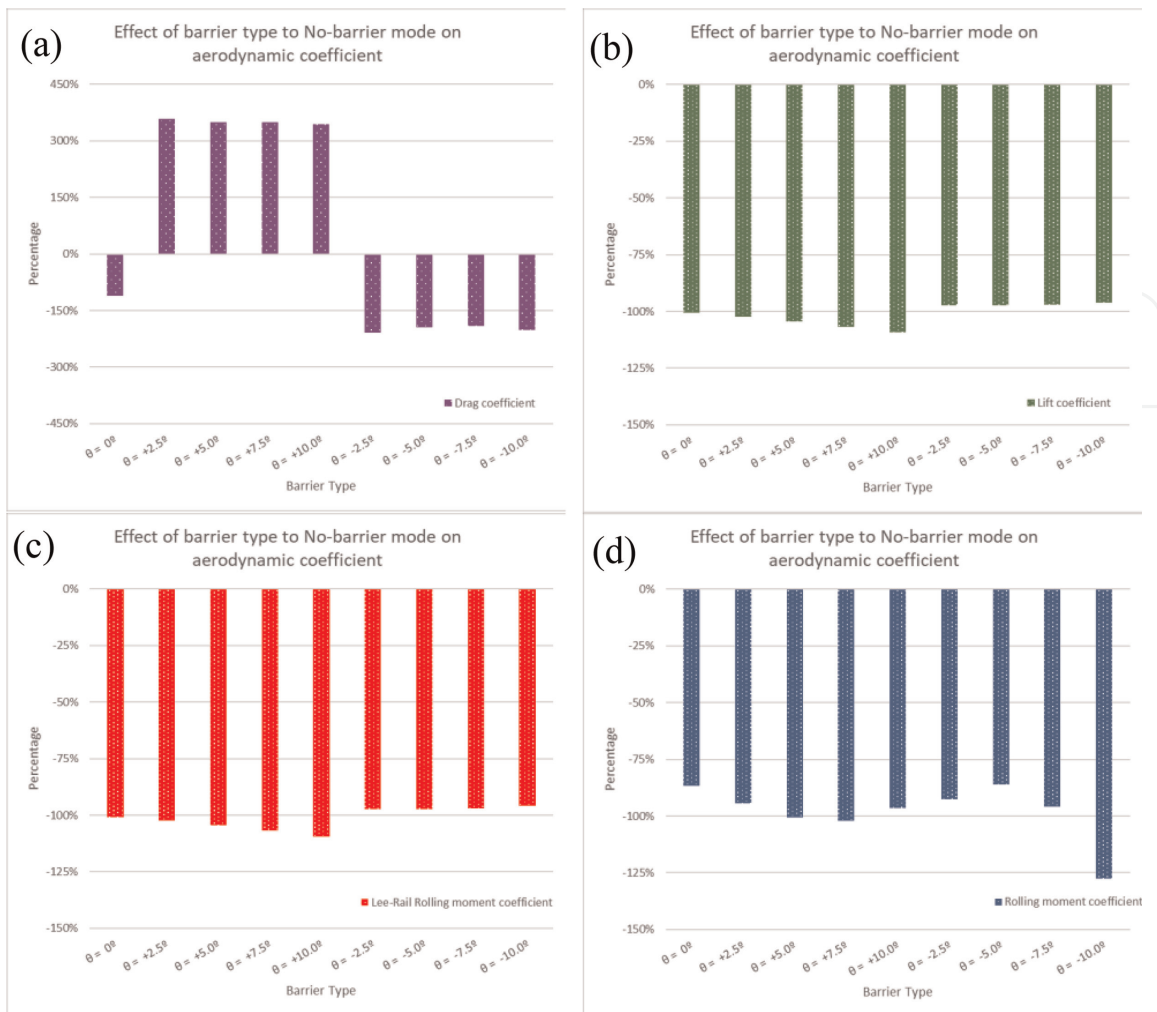


Figure 8. The effects of barrier type on aerodynamic coefficients, (a) drag force coefficient, (b) lift force coefficient, (c) rolling moment coefficient, and (d) lee-rail rolling moment coefficient.

shown in **Figure 8**. In summary, to reduce the aerodynamic coefficients of the train, the barriers with zero inclined angle are the most optimal choice. It appears that the barriers with a positive inclined angle have an inverse effect on the drag coefficient. But the vertical barrier with zero inclined angles has the same effect as the negative ones. As for the lift coefficient, one can find that the existence of any barriers, including the zero inclined angle barriers, leads to a similar influence on the lift coefficient of the train. The same trend also happens for the lee-rail rolling moment coefficient and rolling moment coefficient.

6. Conclusions

In the present work, a 3D numerical model of a train-barrier-crosswind system is adopted to investigate the influence of two inclined barriers on the aerodynamic mechanism of a high-speed train by utilizing the Lattice Boltzmann Method. The influence of barrier inclination angle and direction on the velocity, pressure, turbulence intensity, streamlines, and aerodynamic coefficients are investigated. It has been discovered that utilizing barriers with a positive inclination angle cannot reduce the

drag coefficient. The drag coefficient can be reduced by using barriers with zero or negative angles. When all aerodynamic coefficients are taken into account, barriers with zero or negative inclination angles are the best choice for reduction of its. The value of the rolling moment coefficient reaches a minimum when the inclined angle of the barrier becomes = +5.0°.

IntechOpen

Author details

Masoud Mohebbi^{1*}, Yuan Ma² and Rasul Mohebbi³


1 Iran University of Science and Technology, Tehran, Iran

2 Hong Kong Polytechnic University, Kowloon, China

3 Damghan University, Damghan, Iran

*Address all correspondence to: mohebbi@rail.iust.ac.ir

IntechOpen

© 2023 The Author(s). Licensee IntechOpen. This chapter is distributed under the terms of the Creative Commons Attribution License (<http://creativecommons.org/licenses/by/3.0>), which permits unrestricted use, distribution, and reproduction in any medium, provided the original work is properly cited. 

References

- [1] Schetz JA. Aerodynamics of high-speed trains. *Annual Review of Fluid Mechanics*. 2001;**33**(1):371-414
- [2] He XH, Li H. Review of aerodynamics of high-speed train-bridge system in crosswinds. *Journal of Central South University*. 2020;**27**(4):1054-1073
- [3] Jingping XI, Zhixiang H, Li C. Review of aerodynamic investigations for high speed train. *Mechanics in Engineering*. 2013;**35**(2):1-2
- [4] Barcala MA, Meseguer J. An experimental study of the influence of parapets on the aerodynamic loads under cross wind on a two-dimensional model of a railway vehicle on a bridge. *Proceedings of the Institution of Mechanical Engineers, Part F: Journal of Rail and Rapid Transit*. 2007;**221**(4): 487-494
- [5] Yao Z, Zhang N, Chen X, Zhang C, Xia H, Li X. The effect of moving train on the aerodynamic performances of train-bridge system with a crosswind. *Engineering Applications of Computational Fluid Mechanics*. 2020; **14**(1):222-235
- [6] Zhou L, Liu T, Chen Z, Li W, Guo Z, He X, et al. Comparison study of the effect of bridge-tunnel transition on train aerodynamic performance with or without crosswind. *Wind and Structures*. 2021;**32**(6):597-612
- [7] Guo Z, Liu T, Liu Z, Chen X, Li W. An IDDES study on a train suffering a crosswind with angles of attack on a bridge. *Journal of Wind Engineering and Industrial Aerodynamics*. 2021;**217**: 104735
- [8] Deng E, Yang W, He X, Zhu Z, Wang H, Wang Y, et al. Aerodynamic response of high-speed trains under crosswind in a bridge-tunnel section with or without a wind barrier. *Journal of Wind Engineering and Industrial Aerodynamics*. 2021;**210**:104502
- [9] Guo W, Xia H, Karoumi R, Zhang T, Li X. Aerodynamic effect of wind barriers and running safety of trains on high-speed railway bridges under cross winds. *Wind and Structures*. 2015;**20**(2): 213-236
- [10] Gu H, Liu T, Jiang Z, Guo Z. Experimental and simulation research on the aerodynamic effect on a train with a wind barrier in different lengths. *Journal of Wind Engineering and Industrial Aerodynamics*. 2021;**214**:104644
- [11] Liu T, Chen Z, Zhou X, Zhang J. A CFD analysis of the aerodynamics of a high-speed train passing through a windbreak transition under crosswind. *Engineering Applications of Computational Fluid Mechanics*. 2018; **12**(1):137-151
- [12] Zou S, He X, Wang H. Numerical investigation on the crosswind effects on a train running on a bridge. *Engineering Applications of Computational Fluid Mechanics*. 2020;**14**(1):1458-1471
- [13] Xiang H, Li Y, Chen B, Liao H. Protection effect of railway wind barrier on running safety of train under cross winds. *Advances in Structural Engineering*. 2014;**17**(8):1177-1187
- [14] Yang W, Deng E, Lei M, Zhu Z, Zhang P. Transient aerodynamic performance of high-speed trains when passing through two windproof facilities under crosswinds: A comparative study. *Engineering Structures*. 2019;**188**: 729-744

- [15] Catanzaro C, Cheli F, Rocchi D, Schito P, Tomasini G. High-speed train crosswind analysis: CFD study and validation with wind-tunnel tests. In: International Conference on Engineering Conferences International 2010 Sep 12. Champions: Springer; 2010. pp. 99-112
- [16] Wang M, Li XZ, Xiao J, Zou QY, Sha HQ. An experimental analysis of the aerodynamic characteristics of a high-speed train on a bridge under crosswinds. *Journal of Wind Engineering and Industrial Aerodynamics*. 2018;**177**: 92-100
- [17] Chen S, Doolen GD. Lattice Boltzmann method for fluid flows. *Annual Review of Fluid Mechanics*. 1998;**30**(1):329-364
- [18] Aidun CK, Clausen JR. Lattice-Boltzmann method for complex flows. *Annual Review of Fluid Mechanics*. 2010;**42**:439-472
- [19] Benzi R, Succi S, Vergassola M. The lattice Boltzmann equation: Theory and applications. *Physics Reports*. 1992; **222**(3):145-197
- [20] Mohebbi M, Rezvani MA. Two-dimensional analysis of the influence of windbreaks on airflow over a high-speed train under crosswind using lattice Boltzmann method. *Proceedings of the Institution of Mechanical Engineers, Part F: Journal of Rail and Rapid Transit*. 2018;**232**(3):863-872
- [21] Wang Y, Wang Y, An Y, Chen Y. Aerodynamic simulation of high-speed trains based on the Lattice Boltzmann Method (LBM). *Science in China, Series E Technological Sciences*. 2008;**51**(6): 773-783
- [22] Mohebbi M, Rezvani MA. Analysis of the effects of lateral wind on a high speed train on a double routed railway track with porous shelters. *Journal of Wind Engineering and Industrial Aerodynamics*. 2019;**184**:116-127
- [23] Qian YH, d'Humières D, Lallemand P. Lattice BGK models for Navier-Stokes equation. *EPL (Europhysics Letters)*. 1992;**17**:479
- [24] Bose ST, Park GI. Wall-modeled large-eddy simulation for complex turbulent flows. *Annual Review of Fluid Mechanics*. 2018;**50**:535-561
- [25] Schober M, Weise M, Orellano A, Deeg P, Wetzel W. Wind tunnel investigation of an ICE 3 endcar on three standard ground scenarios. *Journal of Wind Engineering and Industrial Aerodynamics*. 2010;**98**(6-7):345-352